

Development and Characterization of Hybrid Materials Based on Biodegradable PLA Matrix, Microcrystalline Cellulose and Organophilic Silica

Fernanda Abbate dos Santos, Maria Inês Bruno Tavares

Instituto de Macromoléculas Professora Eloisa Mano – IMA, Universidade Federal do Rio de Janeiro – UFRJ

Abstract: The goal of this work was to investigate the production and properties of hybrid materials based on poly(lactic acid) (PLA), employing microcrystalline cellulose (MCC) and organophilic silica (R972) as fillers. The composites were obtained by solution casting to form films. Each nanoparticle was incorporated at 3 wt. %, relative to the polymer matrix. In this experiment, four films were obtained (PLA, PLA/MCC, PLA/R972 and PLA/MCC/R972). The films properties were evaluated by X-ray diffractometry, nuclear magnetic resonance, Fourier transform infrared spectroscopy and mechanical properties. The results showed that each nanoparticle, added individually or both combined, had different effect on the final properties of the films. Microcrystalline cellulose can act as nucleating agent for the crystallization of PLA. Silica promoted an increase in rigidity, due to the strong intermolecular forces, while MCC addition promoted an increase in the molecular mobility of the polymeric chains. The PLA/MCC/R972 film showed the highest crystallinity degree and tensile modulus. This film presented a T_{1H} value between both values found for PLA/MCC and PLA/R972 films. The results indicated that silica R972 could promote a decrease of the surface tension between PLA and cellulose.

Keywords: *Biodegradable polymers, microcrystalline cellulose, silica.*

Introduction

Renewable materials from natural sources have been extensively researched to replace traditional polymers used in various applications^[1,2]. These materials have advantages such as biodegradability, biocompatibility, low toxicity and low cost^[3-6].

Among the main polymers with this characteristic are poly(lactic acid) (PLA) and its copolymers. PLA is biodegradable, aliphatic polyester derived from lactic acid, with similar mechanical properties to polyethylene terephthalate, but it differs from this other polymer for having a significantly lower maximum continuous use temperature. Products based on PLA can be recycled after use either by remelting and processing the material a second time or by hydrolyzing it to lactic acid, which is its basic chemical^[7].

Several studies have been performed, using PLA as polymeric matrix in nanocomposites with fillers such as cellulose, silica and clays^[8-14].

Polymer nanocomposites are a recent alternative to conventionally filled polymers because of their particle size and dispersion. These materials exhibit markedly improved properties when compared to the pure polymers or their traditional composites^[15]. Nanocomposites have properties equivalent or superior to those of conventional composites in many cases and also exhibit unique optical, electrical and magnetic properties^[16]. However, obtaining optimal properties requires good nanoparticle dispersion in the polymer matrix.

The chemical compatibility between nanoparticles and polymer plays a major role in their dispersion in the polymer matrix and the adhesion between these phases.

The aim of this work was to obtain materials based on PLA/cellulose/silica systems and to characterize them by employing conventional techniques such as X-ray diffraction, infrared spectroscopy and tensile testing, and unconventional one, relaxometry, through the determination of proton spin-lattice relaxation time.

For these purposes, hybrid materials based on poly(lactic acid) employing organophilic silica (R972) and microcrystalline cellulose (MCC) were prepared by solution casting in a film form. Each nanoparticle type was incorporated at 3% wt. in relation to the polymer matrix weight. Four films were obtained (PLA, PLA/MCC, PLA/R972 and PLA/MCC/R972). The addition of organophilic silica aimed to improve the compatibility among other components of the system, since the use of cellulose materials with hydrophobic polymers such as PLA promotes weak interaction and results in poor nanoparticle-matrix adhesion.

The materials' preparation and evaluation by X-ray diffraction, infrared spectroscopy and mainly through relaxometry, by determining the proton spin-lattice relaxation time (T_{1H}), which was carried out to understand the materials behavior. The relaxation parameter allows evaluating the molecular dynamics of the samples, according to the changes in the values and in the domain curves of this parameter. In this study, we chosen to

Corresponding author: *Maria Inês Bruno Tavares, Instituto de Macromoléculas Professora Eloisa Mano – IMA, Centro de Tecnologia, Universidade Federal do Rio de Janeiro – UFRJ, Bloco J, Cidade Universitária, Ilha do Fundão, CP 68525, CEP 21945-970, Rio de Janeiro, RJ, Brasil, e-mail: mibt@ima.ufrj.br*

evaluate this parameter through the data obtained from one exponential data. Generally speaking, the decrease in the relaxation parameter is a consequence of an increase in the molecular mobility of chains due to the increase in their freedom^[8,17-19]. Changes in the domain curves such as baseline mean that the samples have an amorphous or non-ordered organization, involving a mixture of more than one chain organization^[8,19].

Experimental

Materials

- PLA Nature Works™ 2002D in pellets form was supplied by Nature works;
- MCC ph102 in the powder form supplied by Viafarma;
- R972, organophilic silica after treated with dimethyldichlorosilane based on hydrophilic silica with a specific surface area of 130 m²/g, was supplied by EVONIK Industries.

Materials development

All materials were prepared by solution casting using CHCl₃ as solvent. Separate solutions of PLA and each nanoparticle were prepared. After stirring each solution for 24 h, the PLA and filler solutions were mixed together for a further 24 h, after which they were cast onto plates and kept in an oven to eliminate the solvent. Four films with different formulations were obtained (see Table 1).

Characterization

X-ray diffraction

X-ray diffraction (XRD) was performed using a Rigaku diffractometer with CuK α radiation ($\lambda = 0.154$ nm, 40 Kv, 120 mA) at room temperature, scanning over the 2θ range from 2° to 40° in 0.05° steps, at a rate of 1°/min.

Nuclear magnetic resonance

The relaxation time was analyzed in a Maran Ultra low field NMR spectrometer (Oxford Instruments), using an 18mm NMR tube, operating at 23 MHz for the hydrogen nucleus. The pulse sequence used to obtain data on spin lattice relaxation time was inversion-recovery (recycle delay – 180° - t - 90° - acquisition data) and the 90° pulse of 4.7ms was calibrated automatically by the instrument's software. The amplitude of the FID was sampled for 40 t data points, ranging from 0.01 to 5000 ms, using 4 scans for each point. The samples were analyzed at 27 °C. The relaxation values and relative intensities were obtained by fitting the exponential data with the aid of the software

Table 1. Formulations of PLA films with nanoparticles and PLA film.

Polymer Matrix (wt.)	Filler (%)	Film
2g PLA	3% R972	PLA/R972
	3% MCC	PLA/MCC
	3%MCC+3%R972	PLA/MCC/R972
	-	PLA film

WINFIT. Distributed exponential fits by plotting the relaxation amplitude versus relaxation time were performed using the software WINDXP. Both softwares come with the low-field NMR spectrometer. The error in the difference values is about 2%.

FTIR

The infrared spectra were recorded with a Varian FTIR model 3100 EXCALIBUR using an HATR accessory from PIKE technologies (Miracle model) with 100 scans and resolution of 4 cm⁻¹. The samples in the film form were cut and deposited on a suitable support. However, organophilic silica and cellulose samples were mixed with potassium bromide (KBr) to form a very fine powder. These powders were compressed into thin pellets and then analyzed.

Mechanical property measurements

Tensile testing was carried out with an Instron Universal Testing Machine, model 4204. Modulus and tensile strength of the films were determined. The tests were performed according to ASTM D882, at 22 °C. Five specimens of each film type were tested.

Results and Discussion

X-ray diffraction

The x-ray diffraction patterns of MCC and silica R972 are shown in Figure 1. The diffractogram of MCC showed a broad peak around 14.9° and two other peaks located at 22.6° and 34.5°. These peaks are characteristic of cellulose I, which is in agreement with the work developed by Rong et al.^[20]. The organically modified Silica R972 showed a halo centered at 22.4°, characteristic of amorphous samples.

The X-ray diffraction patterns of PLA show that the film of this polymer exhibits no peaks, showing an amorphous nature. However, X-ray results for PLA in a pellet form, i.e., before being obtained from solution casting, show that this polymer seems to be semi-crystalline, presenting a peak located at 19.4°, characteristic of PLA (Figure 2). This is in accordance with the results obtained by Almeida et al.^[8].

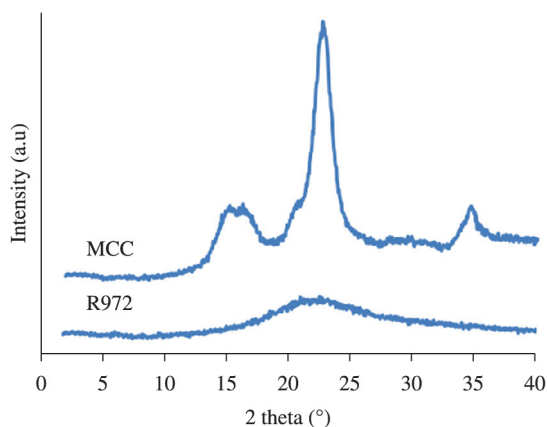


Figure 1. XDR patterns of silica R972 and MCC.

The difference between these XRD results is probably due to the type of polymer molding used in each case. Our films were obtained by solution casting, which does not favor the formation of orderly polymer chains by curbing the chains' approximation, and thus inhibits the development of crystallinity.

The XRD results of the materials are presented in Figure 3. The X-ray diffraction results for the systems PLA/MCC and PLA/MCC/R972 showed peaks related to cellulose and PLA. In the PLA/R972 analysis, no diffraction peak was detected. It's also possible to observe that the silica addition promoted an increase in the intensity of the peak at 22.6°, related to the cellulose.

The crystallinity of the materials was calculated from the X-ray spectra. The results showed that PLA and PLA/R972 films are amorphous while PLA/MCC and PLA/MCC/R972 films exhibited crystallinity (see Table 2).

This effect on the crystallinity of polymer materials is reported in various other studies, in which polymers have been used, like PLA^[2], PCL^[21], PVA^[22] and PHBV^[23]. These results suggest that the effect produced by the cellulose on

the crystallinity of polymer materials is independent of the type of polymer matrix used, and is therefore mainly related to the nature of this filler.

The film PLA/MCC/R972 showed the highest crystallinity degree, which indicates that addition of silica improved the compatibility between the polymer matrix and cellulose.

The silica probably acted by reducing cellulose aggregates, because of the presence of hydroxyl groups that interact with those present at the surface of the cellulose particles, consequently improving dispersion of these particles and affecting the crystallinity by increasing the number of spherulite nuclei. Lu et al.^[22], in their study of the properties of composites based on PVA and microfibrillated cellulose, observed an increase in crystallinity of these materials with the addition of cellulose.

Nuclear magnetic resonance

Table 3 exhibits the proton spin-lattice relaxation times (T_{1H}) determined for all the materials.

The proton spin-lattice relaxation time, determined from one exponential decay, obtained for the PLA film was 650 ms. This T_{1H} value was lower than the parameter value found for PLA pellet (Table 3), which confirms the loss of crystallinity during film formation, already seen from X-ray diffraction.

The T_{1H} value, determined from one exponential decay, for the PLA/MCC system was 580 ms. This result indicates a decrease in this parameter compared to PLA film, as a consequence of an increase in the molecular mobility of the polymer chains with the addition of MCC, due to the new intermolecular interaction formed in the material, causing polymer-polymer chain separations because the MCC chains are well dispersed and distributed in the polymer matrix. The T_{1H} for the film with hydrophobic silica (R972) presented a small increase in the T_{1H} value compared to PLA film, due probably to the increase in the rigidity of the material because of the strong intermolecular forces. Almeida et al.^[8] studied a similar system with PLA and silica and found the same behavior in relation to the T_{1H}

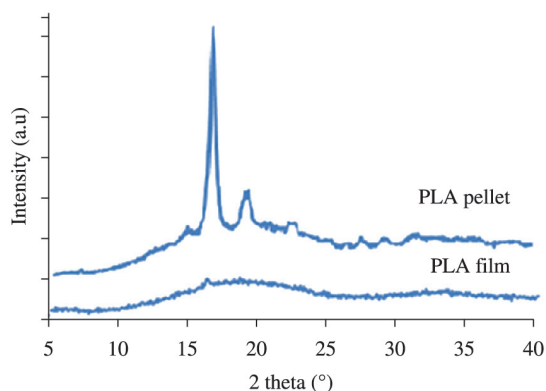


Figure 2. XDR patterns of PLA pellet and PLA film.

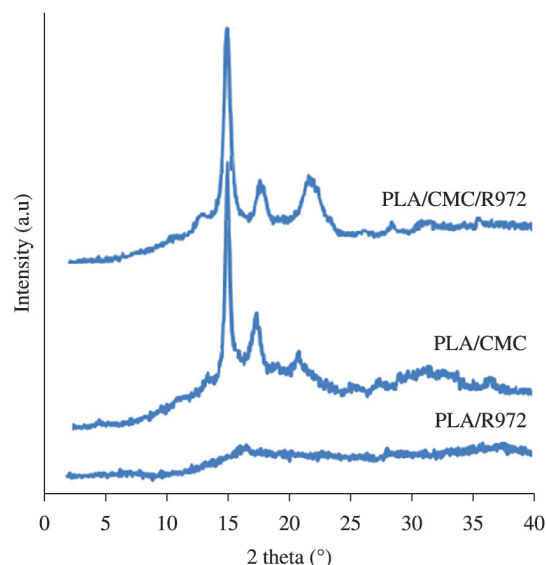


Figure 3. XDR patterns of PLA/MCC/R972 nanocomposites.

Table 2. Crystallinity percent for the films and PLA in the pellet form.

Material	Crystallinity (%)
PLA Pellet	30 ± 0.4
PLA Film	Amorphous
PLA/R972	Amorphous
PLA/MCC	34 ± 0.5
PLA/MCC/R972	39 ± 0.5

Table 3. T_{1H} values for the films and PLA in the pellet form.

Material	T_{1H} (ms) ± 2%
PLA Pellet	690
PLA Film	602
PLA/R972	656
PLA/MCC	580
PLA/MCC/R972	618

parameter, with even lower concentration of organophilic silica.

Figure 4 shows the domain curves for the films. The results for the materials showed no change in the baseline width for the polymer and there was also no displacement of the domains curves, indicating that addition of MCC or silica did not affect the structural organization of the polymer and also that there was good dispersion of the fillers in the matrix.

FTIR

The infrared spectrum for silica (Figure 5) shows a band around 950 cm^{-1} , attributed to Si-O of silanol groups, and also shows strong absorptions at 1175 cm^{-1} and 809 cm^{-1} , assigned to the asymmetric and symmetric stretching of siloxane groups (Si-O-Si)^[24]. The broad absorption band between 400 cm^{-1} and 3000 cm^{-1} corresponds to the vibrations of different basic types at the surface (Si-OH)^[17,25]. The C-H stretch bands of methyl groups derived from dimethyl dichloro silane inserted into silica were observed in the region between $2850\text{--}2990\text{ cm}^{-1}$. Because of the low polarity of methyl groups, this is low-intensity absorption.

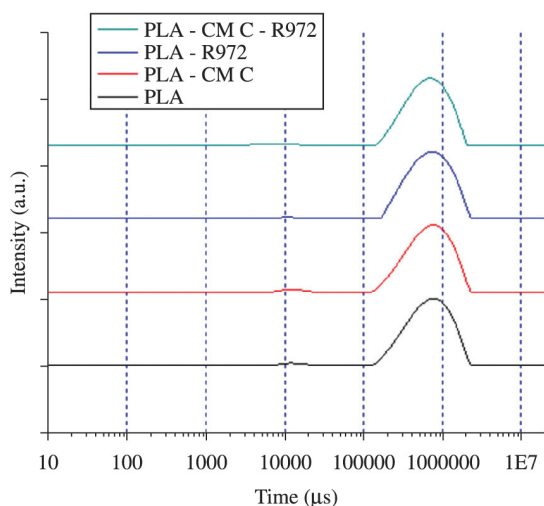


Figure 4. Domain curves for T,H values for the films.

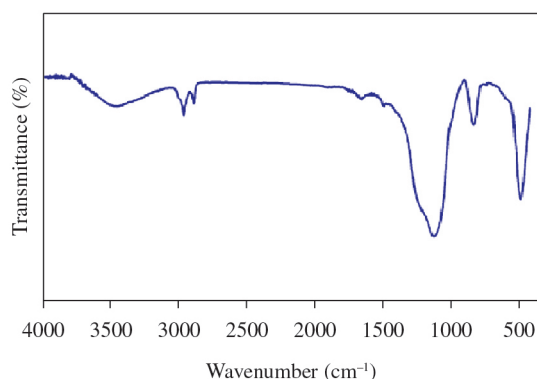


Figure 5. FTIR spectrum obtained from the silica R972.

In the FTIR analysis of the cellulose (Figure 6), the absorption peak in the region around 3400 cm^{-1} is attributed to stretching of OH groups, while that around 2900 cm^{-1} is due to stretching of the CH groups^[26].

Interaction between silica and cellulose might occur due to the hydrogen bonds caused by the hydroxyl groups present in both fillers. In addition, the nanometer-scale silica particles ensure a large specific surface area, allowing greater surface interaction between both particle fillers. Interaction between R972 and PLA chains occurs due to the presence dimethyldichlorosilane, employed as the modifier of the silica. This organophilic modifier provides miscibility between silica nanoparticles and PLA. Thus it is possible that the silica acts by decreasing the surface tension between PLA and cellulose, since it has affinity for both phases.

Mo et al.^[27] studied the interface interactions of amorphous cellulose and silica in nanocomposites. The result showed that the interactions between cellulose and silica increased with the larger radius of silica nanocomposites. They also found that cellulose chains were more attracted to the modified silica surfaces due to the induction force and hydrogen bonds between cellulose chains and silica surfaces.

Xu et al.^[28] reported that in NR nanocomposites, materials containing silanized cellulose and silica present good dispersion of the filler in the matrix and strong filler-matrix interfacial interaction.

Mechanical property measurements

The tensile strength and the tensile modulus of the prepared films are presented in Figure 7 and 8, respectively. The PLA/MCC film exhibited a reduction in the tensile strength compared to the value found in the PLA film analysis. On the other hand, the tensile strength values for PLA and PLA/R972 films did not present significant difference. However, the PLA/MCC/R972 film showed an improvement in the tensile strength compared to the pure material. PLA/R972 and PLA/MCC films showed reductions in the tensile strength of about 4% and 39%, respectively, compared to the value found for the pure PLA film. And PLA/MCC/R972 film presented an increase of about 8% in tensile strength.

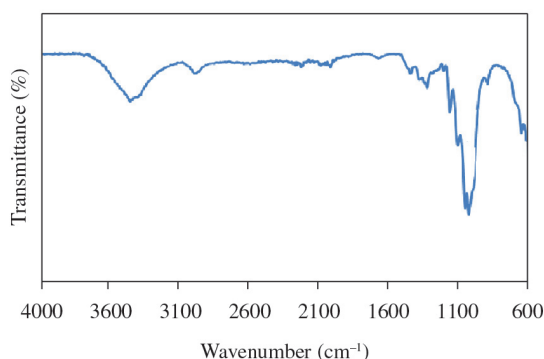


Figure 6. FTIR spectrum obtained from the MCC.

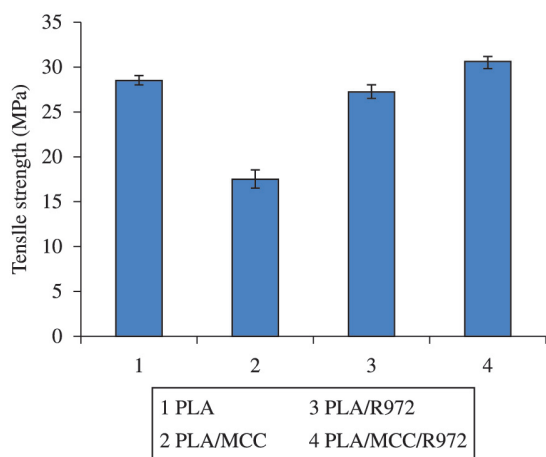


Figure 7. Tensile Strength of the PLA, PLA/MCC, PLA/R972 and PLA/MCC/R972 films.

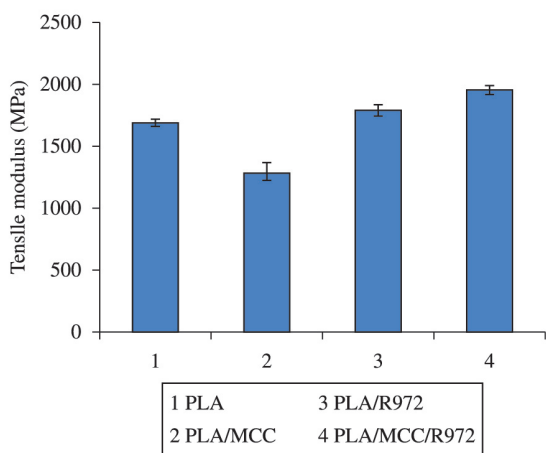


Figure 8. Tensile Modulus of PLA, PLA/MCC, PLA/R972 and PLA/MCC/R972 films.

This mechanical behavior observed for the PLA/MCC film can be explained by the poor MCC dispersion and the presence of larger cellulose particle agglomerates in the polymeric matrix. On the other hand, the addition of silica R972 promoted a decrease in the tensile strength. However, the concomitant addition of the two types of filler promoted the highest tensile strength. The tensile strength of the PLA/MCC/R972 film was 75% higher than for the PLA/MCC film. The addition of both fillers together promoted formation of materials with synergetic properties,

The increase in tensile strength observed in the sample prepared with R972 compared to the film without the addition of silica indicates a better stress transfer from the matrix to the reinforcement at the filler-polymer interface.

Similar behavior was observed regarding tensile modulus. The addition of MCC promoted a substantial decrease in this property, whereas the addition of silica and cellulose together promoted an increase in the tensile modulus of the PLA/MCC/R972 film compared to the pure polymer film. However, the addition of only the silica produced a very small increase in the tensile modulus value.

In more detail, PLA/R972 and PLA/MCC/R972 showed 6% and 16% improvements in this property compared to the value found for the pure PLA film. PLA/MCC film presented a decrease in the tensile modulus of about 24%. However, the tensile modulus to the PLA/MCC/R972 film was 50% higher than that of the PLA/MCC film.

Petersson & Oksman^[29] reported a similar result in their study of PLA/MCC films obtained by solution casting. The authors observed a decrease in modulus from 1700 MPa for neat PLA film to 1500 MPa in the PLA film containing 5% wt. MCC. Nevertheless, Oksman et al.^[30], studying PLA/MCC based materials obtained by extrusion, reported an increase in tensile modulus but a loss in tensile strength of the material with increasing content of MCC. The ability to strengthen microcrystalline cellulose may be associated with factors such as matrix/cellulose system and processing conditions.

Abdelmouleh et al.^[31] produced materials based on unsaturated polyester and phenolic resin reinforced with cellulose fibers using four different organoalcoxilanes as coupling agents. The materials produced with these coupling agents showed better performance compared to those in the module where no procedure was used to improve compatibility of phases.

Regarding the silica addition, the results showed that only the use of R972 was not able to produce a significant increment in the tensile modulus, but when both silica and cellulose were added together, the modulus exhibited its highest value, due to the synergetic effect of the filler and good dispersion and distribution of both fillers in the polymeric matrix. This indicates that silica R972 acted by reducing the interfacial tension between the PLA and MCC, which probably occurred due to the presence of hydroxyl group on the silica surface that interacted through hydrogen bonds with cellulose, and also due to the presence of the organophilic modifier R972, which might have limited the interaction between silica and PLA.

Conclusions

The XRD studies showed that cellulose can act as nucleating agent on the crystallization type of PLA. The use of silica as the only nanoparticle does not have any effect on the crystallinity type of the PLA; but when silica is added together with cellulose a more pronounced increase in the crystallinity degree is observed, due to the synergetic effects of the two nanoparticles. Silica is also able to reduce cellulose aggregates. Therefore, the efficiency of nucleation is associated with not only the chemical nature of the particle, but also with the increase of contact surface of cellulose and silica.

NMR analyses showed that the cellulose and silica, when they are added alone, exert opposite effects on the T_{1H} parameter; while the cellulose increases the molecular mobility in the polymer matrix, the silica increases the rigidity. The film containing both types of nanoparticles the T_{1H} parameter presented intermediate value between

polymer film and the polymer film containing both silica and cellulose.

FTIR analysis confirmed that silica has groups, which can interact with cellulose and polymer groups, decreasing the surface tension between PLA and cellulose. This behavior can be associated with the higher crystallinity when both nanoparticles are added together and justifies the increased stiffness of the film compared to the film with cellulose.

Neither of the two nanoparticles used alone was able to produce an increase in the mechanical properties. Only by using the silica and microcrystalline cellulose together was an improvement in the mechanical performance.

The crystallinity degree calculations for the films explain the behavior of results found for the tensile modulus analysis, since the film with highest crystallinity degree also presented the highest value of tensile modulus.

The results obtained from the four analytical techniques used indicate better dispersion of the cellulose in the polymer matrix in the presence of silica and increased filler-matrix interaction, as expected. The use of organophilic silica proved to be determinant factor to obtain gains on the studied properties.

References

1. Bilbao-Sainz, C.; Bras, J.; Williams, T.; Sénechal, T. & Orts, W. - Carbohydr. Polym., **86**, p.1549 (2011). <http://dx.doi.org/10.1016/j.carbpol.2011.06.060>
2. Suryanegara, L.; Nakagaito, A. N. & Yano, H. - Compos. Sci. Technol., **69**, p.1187 (2009). <http://dx.doi.org/10.1016/j.compscitech.2009.02.022>
3. Davis, G. & Song, J. H. - Ind. Crop. Prod., **23**, p.147 (2006). <http://dx.doi.org/10.1016/j.indcrop.2005.05.004>
4. Mecking, S. - Angew. Chem. Int. Ed. Engl., **43**, p.1078 (2004). PMID:14983440. <http://dx.doi.org/10.1002/anie.200301655>
5. Mohanty, A. K.; Misra, M. & Drzal, L. T. - J Polym. Environ., **10**, p.19 (2002). <http://dx.doi.org/10.1023/A:1021013921916>
6. Mohanty, A. K.; Misra, M. & Hinrichsen, G. - Macromol. Mater. Eng., **276-277**, p.1 (2000). [http://dx.doi.org/10.1002/\(SICI\)1439-2054\(20000301\)276:1<1::AID-MAME1>3.0.CO;2-W](http://dx.doi.org/10.1002/(SICI)1439-2054(20000301)276:1<1::AID-MAME1>3.0.CO;2-W)
7. Pang, X.; Zhuang, X.; Tang, Z. & Chen, X. - J. Biotechnol., **5**, p.1125 (2010).
8. Almeida, A. S.; Tavares, M. I. B.; Silva, E. O.; Cucinelli Neto, R. P. & Moreira L. A. - Polym. Test., **31**, p.267 (2012).
9. Jonoobi, M.; Mathew, A. P.; Abdi, M. M.; Makinejad, M. D. & Oksman, K. J. - Polym. Environ., **20**, p.991 (2012). <http://dx.doi.org/10.1007/s10924-012-0503-9>
10. Li, Y.; Han, C.; Bian, J.; Han, L.; Dong, L. & Gao, G. - Polym. Compos., **33**, p.1719 (2012). <http://dx.doi.org/10.1002/pc.22306>
11. Najafi, N.; Heuzey, M. C. & Carreau, P. J. - Compos Sci Technol., **72**, p.608 (2012). <http://dx.doi.org/10.1016/j.compscitech.2012.01.005>
12. Nakagaito, A. N.; Fujimura, A.; Sakai, T.; Hama, Y. & Yano, H. - Comp Sci. Techn., **69**, p.1293 (2009). <http://dx.doi.org/10.1016/j.compscitech.2009.03.004>
13. Nam, J. Y.; Ray, S. S. & Okamoto, M. - Macromol., **36**, p.7126 (2003). <http://dx.doi.org/10.1021/ma034623j>
14. Tingaut, P.; Zimmermann, T. & Lopez-Suevos F. - Biomacromol., **11**, p.454 (2010). PMID:20025270. <http://dx.doi.org/10.1021/bm901186u>
15. Farsani, R. E.; Nasab, Z. H.; Khalili, S. M. R. & Soleimani, N. - Adv. Mat. Res., **448**, p.567 (2012). <http://dx.doi.org/10.4028/www.scientific.net/AMR.488-489.567>
16. Medeiros, V. N.; Araújo, E. M.; Maia, L. F.; Pereira, O. D.; Arimateia, R. R. & Paz, R. A. - Polímeros, **18**, p.302 (2008).
17. Vanderhart, D. L.; Asano, A. & Gilman, J. W. - Chem. Mater., **13**, p.3781 (2001). <http://dx.doi.org/10.1021/cm0110775>
18. Monteiro, M. S. S. B.; Cucinelli Neto, R. P.; Santos, I. C. S.; Silva, E. O. & Tavares M. I. B. - J. Mat. Res. **15**, p.825 (2012). <http://dx.doi.org/10.1590/S1516-14392012005000121>
19. Monteiro, M. S. S. B.; Silva, E. O.; Rodrigues, C. L.; Cucinelli Neto, R. P. & Tavares, M. I. B. - J. Nanosci. Nanotechnol., **12**, p.7307 (2012). PMID:23035469. <http://dx.doi.org/10.1166/jnn.2012.6431>
20. Rong, M. Z.; Zhang, M. Q.; Liu, Y.; Yang, G. C. & Zeng, H. M. - Compos. Sci. Technol., **61**, p.1427 (2001).
21. Siqueira, G.; Bras, J. & Dufresne, A. - Biomacromol., **10**, p.425 (2009). PMID:19113881. <http://dx.doi.org/10.1021/bm801193d>
22. Lu, J.; Wang, T. & Drzal, L.T. - Compos Part A Appl Sci Manuf., **39**, p.738 (2008). <http://dx.doi.org/10.1016/j.compositesa.2008.02.003>
23. Jiang, L.; Morelius, E.; Zhang, J.; Wolcott, M. & Holbery, J. J. - Compos. Mater., **42**, p.2629 (2008).
24. Lee, E. C.; Mielewski, D. F. & Baird; R. J. - Polym. Eng. Sci., **44**, p.1773 (2004). <http://dx.doi.org/10.1002/pen.20179>
25. Pereira, A. - "Micro-extração em fase sólida de Cu(II) e Cd(II) em meio aquoso utilizando sílica organicamente modificada para quantificação por espectrometria de absorção atômica", Dissertação de Mestrado, Universidade Estadual Paulista, Ilha Solteira, Brasil (2009).
26. Oh, S. Y.; Yoo, D. I.; Shin, Y.; Kim, H. C.; Kim, H. Y.; Chung, Y. S.; Park, W. H. & Youke, J. H. - Carbohydr. Res., **340**, p.2376 (2005). PMID:16153620. <http://dx.doi.org/10.1016/j.carres.2005.08.007>
27. Mo, Z. L.; Qiao, L. J.; Chen, H.; Guo, R. B.; Sun, Y. L. & Li, H. J. - J Mater. Sci. Eng., **2**, p.17 (2008).
28. Xu, S. H.; Gu, J.; Luo, Y. F. & Jia, D. M. - Express Polym. Lett., **6**, p.14 (2012). <http://dx.doi.org/10.3144/expresspolymlett.2012.3>
29. Petersson, L. & Oksman, K. J. - ACS Symp. Ser., **938**, p.132 (2006). <http://dx.doi.org/10.1021/bk-2006-0938.ch010>
30. Oksman, K.; Mathew, A. & Sain, M. - J Appl. Polym. Sci., **101**, p.300 (2006). <http://dx.doi.org/10.1002/app.23346>
31. Abdelmouleh, M.; Boufi, S.; Belgacem, M. N.; Dufresne, A.; Gandini, A. - J Appl. Polym. Sci., **98**, p.974 (2005). <http://dx.doi.org/10.1002/app.22133>

Received: Dec. 30, 2013
Revised: May 05, 2014
Accepted: May 23, 2014